

---

# On Multi-objective Policy Optimization as a Tool for Reinforcement Learning

---

Abbas Abdolmaleki\*, Sandy H. Huang\*, Giulia Vezzani, Bobak Shahriari,  
Jost Tobias Springenberg, Shruti Mishra, Dhruva TB, Arunkumar Byravan,  
Konstantinos Bousmalis, András György, Csaba Szepesvári,  
Raia Hadsell, Nicolas Heess, Martin Riedmiller  
DeepMind  
London, UK  
aabdolmaleki, shuang@deepmind.com

## Abstract

Many advances that have improved the robustness and efficiency of deep reinforcement learning (RL) algorithms can, in one way or another, be understood as introducing additional objectives, or constraints, in the policy optimization step. This includes ideas as far ranging as exploration bonuses, entropy regularization, and regularization toward teachers or data priors when learning from experts or in offline RL. Often, task reward and auxiliary objectives are in conflict with each other and it is therefore natural to treat these examples as instances of multi-objective (MO) optimization problems. We study the principles underlying MORL and introduce a new algorithm, Distillation of a Mixture of Experts (DiME), that is intuitive and scale-invariant under some conditions. We highlight its strengths on standard MO benchmark problems and consider case studies in which we recast offline RL and learning from experts as MO problems. This leads to a natural algorithmic formulation that sheds light on the connection between existing approaches. For offline RL, we use the MO perspective to derive a simple algorithm, that optimizes for the standard RL objective plus a behavioral cloning term. This outperforms state-of-the-art on two established offline RL benchmarks.

## 1 Introduction

Deep reinforcement learning (RL) algorithms have solved a number of challenging problems, including in games [24, 47], simulated continuous control [15, 36], and robotics [19, 31]. The standard RL setting appeals through its simplicity: an agent acts in the environment and can discover complex solutions simply by maximizing the longer-term discounted reward that indicates success. In practice, however, the situation is often more complicated: for instance, without a carefully crafted reward function or sophisticated exploration strategy, learning may not be able to proceed, and even then finding a good policy may require hundreds of millions of environment interactions.

A number of strategies have been developed to mitigate shortcomings of the pure RL paradigm. This includes strategies to regularize the final solution, for instance by maximizing auxiliary rewards [17] or the entropy of the policy [25, 14]. Other strategies facilitate exploration, for instance via demonstrations [6], shaping rewards [29], exploration bonuses [4, 35], or guidance from a pre-trained teacher policy, known as kickstarting [44, 10]. There are also strategies for reusing old environment interactions, in the extreme case enabling agents to learn solely from a fixed dataset, known as offline RL [8, 13]—in which case regularization is needed to ensure the learned policy is well supported by the data distribution (i.e., it stays close to the policies that generated the data).

---

\*equal contribution

These approaches may seem quite different at first glance, but they can all be understood as introducing additional objectives, or constraints, in the policy optimization step. Since these additional objectives are usually in conflict with the goal of maximizing the environment reward, they require the user to balance, or *trade off* their influence with that of the primary goal of maximizing reward. Typically this trade-off is treated as a hyperparameter to optimize. This process, however, can be computationally expensive and time consuming, and usually no single trade-off works best for all tasks.

In this paper we take an alternative perspective: we treat the trade-off as an integral part of the problem and consider multi-objective optimization techniques for tackling fundamental challenges in deep RL. This perspective has several advantages. First, it provides a better understanding of the principles underlying existing algorithms. Second, it motivates treating the trade-off as a key parameter to optimize for or search over. Third, it opens the door to using alternate multi-objective approaches. We demonstrate these advantages in two case studies, on offline RL and kickstarting.

Our main contributions are as follows:

- We introduce a scale-invariant multi-objective RL algorithm, called Distillation of a Mixture of Experts (DiME), that is an intuitive and flexible alternative to existing approaches. We show that linear scalarization and DiME solve the same multi-objective problem (Sec. 4.1) and derive a new method for offline RL that strongly outperforms state-of-the-art (Sec. 6) This method is simple and intuitive: it optimizes for the standard RL objective, plus a behavioral cloning term.
- We derive the policy loss of existing approaches, in both offline RL and kickstarting, from the multi-objective perspective (Sec. 5), showing that they rely on linear scalarization and providing a deeper understanding of what these approaches are optimizing.
- We explore either learning the trade-off or conditioning the policy on it, to improve computational efficiency. This works for both DiME and linear scalarization (Sec. 6).

## 2 Related Work

**Multi-Objective RL.** Multi-objective RL algorithms train policies for environments with multiple sources of reward. There are two broad categories of algorithms: single-policy and multi-policy [50]. The former category involves training a policy that is optimal for a single preference trade-off across reward sources. One common technique is to use the trade-off to combine the rewards into a single scalar reward to then use standard RL algorithms for optimization [40]. Typically linear scalarization is used, but it is sensitive to reward scales and cannot always find optimal solutions [7]. Although non-linear scalarizations exist [49, 51, 12], these are hard to combine with value-based RL. Instead of scalarizing the rewards, recent work proposed a constrained optimization approach, MO-MPO [2].

Multi-policy approaches seek to find a set of policies that cover the Pareto front. Various techniques exist, for instance repeatedly calling a single-policy approach with strategically-chosen trade-off settings [41, 27, 55], simultaneously learning a set of policies by using a multi-objective variant of Q-learning [26, 39, 54], learning a manifold of policies in parameter space [32, 33], or combining single-policy approaches with an overarching objective [53].

In contrast to prior work, here we consider objectives that are not only sources of environment reward, but also learning- or regularization-focused objectives such as staying close to a behavioral prior. Like MO-MPO, our multi-objective RL algorithm DiME computes a local expert for each objective, and then distills these into an updated policy. Whereas MO-MPO incorporates the trade-off in computing the per-objective experts, DiME incorporates the trade-off in the distillation step, which is more intuitive and flexible. We expand on this in Sec. 4.

**Offline RL and Kickstarting.** Our case studies in this work will involve two related learning problems: that of offline (or batch) reinforcement learning [22] and that of kickstarting [44].

In offline RL, the goal is to learn a policy from a given, fixed dataset of transitions. While classical off-policy RL algorithms can be used, they perform worse than bespoke algorithms [9]. This is likely due to the extrapolation errors incurred when learning a Q-function—naïve policy optimization could optimistically exploit such errors and produce arbitrarily poor policies. Therefore, many existing approaches attempt to constrain the policy optimization to stay close to the samples present in the available dataset [37, 28, 46, 52]. In this work, we use the proximity to the dataset as an additional objective in a multi-objective RL problem. We show that from this perspective, existing approaches

in the literature boil down to a linear scalarization of the objectives of (i) return maximization and (ii) maximizing the log-density ratio of the current policy and offline data distribution (a common measure of proximity in imitation learning for distribution matching [20]).

While offline RL assumes a dataset of interactions with the environment, when kickstarting an agent (or student) we usually have access to an expert (or teacher) policy’s functional form. Kickstarting typically happens in an online setting, where the student policy is interacting with the desired environment. In this case, using distillation (or mimicking) is feasible [43, 34]: these approaches use the teacher network’s logits to minimize the cross-entropy between the teacher and student policies.

### 3 Background

We consider the RL problem defined by a Markov Decision Process (MDP). An MDP consists of states  $s \in \mathcal{S}$  and actions  $a \in \mathcal{A}$ , an initial state distribution  $p(s_0)$ , transition probabilities  $p(s_{t+1}|s_t, a_t)$ , a reward function  $r(s, a) \in \mathbb{R}$ , and a discount factor  $\gamma \in [0, 1)$ . We define the policy  $\pi_\theta(a|s)$  as a state-conditional distribution over actions, parametrized by  $\theta$ . Together with the transition probabilities, this gives rise to a state visitation distribution  $\mu(s)$ . The action-value function is the expected return (i.e., cumulative discounted reward) from choosing action  $a$  in state  $s$  and then following policy  $\pi$ :  $Q^\pi(s, a) = \mathbb{E}_\pi[\sum_{t=0}^{\infty} \gamma^t r(s_t, a_t) | s_0 = s, a_0 = a]$ . We represent this function using the expression  $Q^\pi(s, a) = \mathbb{E}_{s' \sim p}[r(s, a) + \gamma V^\pi(s')]$ , where  $V^\pi(s) = \mathbb{E}_{a \sim \pi}[Q^\pi(s, a)]$  is the value function of  $\pi$ .

#### 3.1 Multi-Objective Reinforcement Learning

We apply the policy iteration family of algorithms to the task of multi-objective RL. These algorithms consist of repeatedly alternating two steps: policy evaluation and policy improvement.

In the policy evaluation step, we evaluate the current policy  $\pi_{\theta_i}$  by training a separate Q-function for every objective that requires bootstrapping, according to Q-decomposition [42]. Any policy evaluation algorithm can be used to learn these Q-functions. We use distributional Q learning and include details in the appendix.

Meanwhile, in the policy improvement step, given the previous policy  $\pi_{\theta_i}$  and associated Q-functions  $\{Q_k^i\}_{k=1}^K$ , we aim to improve the policy for a given state visitation distribution  $\mu$ . Note that not all the objective functions in this set are necessarily learned via bootstrapping in the policy evaluation step, but we denote them as  $Q_k$  as well to lighten notation.<sup>2</sup> This paper proposes a new algorithm to perform policy improvement in the presence of multiple objectives, so we provide further background on the policy improvement step in the following section, first focusing on the single-objective setting.

#### 3.2 (Single-Objective) Policy Improvement

We consider the view introduced by Ghosh et al. [11], that decomposes policy improvement into two steps: 1) find an improved policy with respect to an objective (e.g., a learned Q-function), and 2) project this improved policy back into the space of allowed policies, which is usually a parametric space that facilitates sampling. These two steps are performed iteratively.

**Improvement.** In this step, we find an improved policy  $q(a|s)$  that optimizes the KL-regularized RL objective, staying close to the current iterate  $\theta_i$  (we shorten  $\pi_{\theta_i}$  to  $\pi_i$  when clear from context):

$$F(q; \theta_i) = \mathbb{E}_{\substack{s \sim \mu \\ a \sim q}} [Q(s, a)] - \eta \mathbb{E}_{s \sim \mu} [\text{KL}(q(\cdot|s) \| \pi_i(\cdot|s))]. \quad (1)$$

The known nonparametric solution to this is  $q(a|s) \propto \pi_i(a|s) \exp(Q(s, a)/\eta)$  [38, 1]. However, this improved policy  $q$  is not necessarily in the allowed family of policies; for instance it may not allow for efficient sampling.

**Projection.** Next, we project the improved policy  $q$  to the space of parametric policies by minimizing

$$J(\theta) = \mathbb{E}_{s \sim \mu} \text{KL}(q(\cdot|s) \| \pi_\theta(\cdot|s)), \quad (2)$$

to get the next iterate  $\theta_{i+1} = \text{argmin}_\theta J(\theta)$ . Note that if we instead use a parametric  $q = \pi_\theta$  in the improvement step, then we can forgo the projection and the algorithm reduces to the policy gradient.

<sup>2</sup>As we focus on policy improvement in this paper, we drop the superscript  $i$  on  $Q_k^i$ , always assuming the latest iterate of the policy evaluation algorithm.

### 3.3 Multiple Objectives and Linear Scalarization

Suppose that we want our policy to improve with respect to  $K$  objectives instead. For the objective of maximizing environment return, the evaluation function is the usual learned Q-function. Recall, however, that for the other objectives,  $Q_k$  need not necessarily be a Q-function. A policy is *Pareto-optimal* if there is no other policy that obtains better performance for one objective without decreasing performance for another.

Let  $\{\alpha_k\}_{k=1}^K$  define a convex preference trade-off across objectives such that  $\sum_k \alpha_k = 1$  and all  $\alpha_k \geq 0$ . Larger values of  $\alpha_k$  translate to objective  $k$  being more important and should lead to increased influence of objective  $k$  on the policy optimization.

In the linear scalarization approach, this trade-off setting is used to produce a scalar reward via a convex combination of the objectives, which leads to the following nonparametric solution, analogous to that of Eq. (1):  $q(a|s) \propto \pi_i(a|s) \exp(\sum_k \alpha_k Q_k(s, a)/\eta)$ . The projection step is then identical to the single objective scenario, meaning that in linear scalarization, the trade-offs  $\{\alpha_k\}$  are taken into account in the improvement (rather than projection) step.

## 4 Distilled Mixture of Experts

In contrast to linear scalarization, with the distilled mixture of experts (DiME), we propose to compute a separate  $q_k$  per objective. In other words, DiME optimizes (1) separately for each objective, where the nonparametric solution is analogously  $q_k(a|s) \propto \pi_i(a|s) \exp(Q_k(s, a)/\eta_k)$ . DiME then incorporates the tradeoffs in the projection (rather than improvement) step as follows

$$J_{\text{DiME}}(\theta) = \mathbb{E}_{s \sim \mu} \sum_{k=1}^K \alpha_k \text{KL}(q_k(\cdot|s) \parallel \pi_\theta(\cdot|s)). \quad (3)$$

In Sec. 4.1, we derive both DiME and linear scalarization from a unified multi-objective policy improvement problem. The main advantage of DiME is that combining the objectives in the projection step enables combining them in a *scale-invariant* way<sup>3</sup>, so that the trade-offs  $\{\alpha_k\}$  directly control the influence of the objectives. In contrast, the linear scalarization approach of combining the objectives in the improvement step means that not only the trade-offs, but also the scales of the  $Q_k$  will influence the contribution of each objective  $k$ . DiME also enables decoupling the improvement per objective.

In some cases we may not know the best preference trade-offs for a given task, or it might be difficult to evaluate trade-offs during training (as is the case for offline RL). To address this, we propose training trade-off-conditioned policies. When acting in the environment, at the start of each episode, we select a tradeoff and then condition the policy on it for the whole episode.

To train this trade-off-conditioned policy, we augment the state with normalized trade-off vectors  $\underline{\alpha} \in \mathbb{R}_+^K$ , sampled from some distribution  $\nu$ . We optimize the policy for the following objective:

$$J_{\text{DiME}}^\alpha(\theta) = \mathbb{E}_{\substack{s \sim \mu \\ \underline{\alpha} \sim \nu}} \sum_{k=1}^K \alpha_k \text{KL}(q_k(\cdot|s, \underline{\alpha}) \parallel \pi_\theta(\cdot|s, \underline{\alpha})), \quad (4)$$

where  $q_k(a|s, \underline{\alpha}) \propto \pi_i(a|s, \underline{\alpha}) \exp(Q_k(s, a, \underline{\alpha})/\eta_k)$ . Note that in order to evaluate this policy, we must also learn a trade-off-conditioned Q-function  $Q_k(s, a, \underline{\alpha})$ . Appendix A contains more details.

**Comparison with MO-MPO.** MO-MPO also proposes to optimize for a separate  $q_k$  per objective, but like linear scalarization, it incorporates the trade-offs in the improvement (rather than projection) step, by choosing a different KL-constraint between each  $q_k$  and the policy iterate  $\pi_i$ . The trade-offs correspond to the thresholds of the divergence constraints. One disadvantage is that the improvement operator used for  $q_k$  must be able to meet this constraint exactly—this is true for the known nonparametric solution, but not the case for policy gradient approaches, for example. In contrast, since in DiME the trade-offs are incorporated in the projection step instead, any improvement operator can be used to obtain  $q_k$ . In addition, the trade-offs in DiME are more interpretable than those in MO-MPO, since they are weights on local experts  $q_k$ , rather than KL-divergence constraints.

<sup>3</sup>As long as the improvement step is scale-invariant, which is the case for the known nonparametric solution if we optimize for the temperature  $\eta$  to meet a constraint on the KL-divergence (e.g., as is done in MPO [1]).

#### 4.1 Multi-Objective RL as Probabilistic Inference

In this section we present a unifying derivation of both linear scalarization and DiME, relying on the *RL as inference* framework. Consider a binary random variable  $R$  indicating a policy improvement event. Policy optimization then corresponds to maximizing the marginal likelihood  $\mathbb{E}_\mu \log p_\theta(R|s)$  with respect to  $\theta$ . Employing the expectation-maximization (EM) algorithm and assuming a conditional probability  $p(R|s, a) \propto \exp(Q(s, a)/\eta)$ , we can recover many algorithms in the literature [23]. Let us instead define a separate indicator  $R_k$  for each objective, with similarly defined conditional probabilities and consider the following weighted log-likelihood objective:

$$F(\theta) = \mathbb{E}_\mu \log \prod_{k=1}^K p_\theta(R_k|s)^{\alpha_k} = \sum_{k=1}^K \alpha_k \mathbb{E}_\mu \log p_\theta(R_k|s), \quad (5)$$

where  $\mathbb{E}_\mu$  is a shorthand for  $\mathbb{E}_{s \sim \mu}$  and  $\alpha_k$  specify a convex preference trade-off across objectives. This generalization has a few nice properties. First, when all objectives are equally preferred, the  $\alpha_k$  are all equal and it reduces to a straightforward probabilistic factorization of independent events:  $p(\{R_k\}_{k=1}^K) = \prod_k p(R_k)$ . Second, any vanishing  $\alpha_k$  leads to an objective being ignored.

**Linear scalarization.** Let us first simply apply the EM algorithm: we introduce a variational distribution  $q(a|s)$  and use it to decompose (5) into:

$$F(\theta) = F_{\text{LS}}(\theta; q) = \sum_{k=1}^K \alpha_k \mathbb{E}_\mu [\text{KL}(q(a|s) \parallel p_\theta(a|R_k, s)) - \text{KL}(q(a|s) \parallel p_\theta(R_k, a|s))], \quad (6)$$

where  $p_\theta(a|R_k, s)$  is the improved policy  $\pi_\theta(a|s)$  that we seek. We alternate optimizing  $F_{\text{LS}}$  with respect to  $q$  and  $\theta$ , respectively, keeping the other fixed. These steps correspond to the improvement and projection steps (or E- and M-step) that have already been introduced. Furthermore, with this choice of variational distribution, the improvement step corresponds to Equation (1) with a linearly scalarized objective  $\sum_k \alpha_k Q_k(s, a)$  replacing  $Q(s, a)$ . The projection step is identical to (2).

**Distilled Mixture of Experts.** Instead we propose to optimize *a separate*  $q_k$  for each  $\log p_\theta(R_k|s)$ .

$$F(\theta) = F_{\text{DiME}}(\theta; \{q_k\}) = \sum_{k=1}^K \alpha_k \mathbb{E}_\mu [\text{KL}(q_k(a|s) \parallel p_\theta(a|R_k, s)) - \text{KL}(q_k(a|s) \parallel p_\theta(R_k, a|s))] \quad (7)$$

Keeping  $\theta = \theta_i$  fixed in the improvement (E-step) leads to  $K$  copies of the canonical improvement step exactly as it appears in (1), each with its own  $Q_k(s, a)$ . The projection step then reveals the update equation we already introduced in (3).

These derivations, expanded in more detail in Appendix B, reveal that *both standard linear scalarization and our method optimize the exact same information-theoretic objective*, both employing EM and simply differing only in their choice of variational decomposition.

## 5 Case Studies

We focus on making use of behavioral priors in deep RL. The goal is to use the prior to enable more efficient optimization of the task reward. The prior is given as sampled experiential data (offline RL) or as a parametric policy, that can be queried for actions and probabilities.

We model this as a multi-objective problem with two objectives: the task return and staying “close” to the prior. This is a general framework—one can choose how to formalize the mathematical objective functions corresponding to each objective; we choose to use the following objective functions:

1. for the task return: the task Q-function  $Q(s, a)$  learned via bootstrapping
2. for staying close to the behavioral prior: the log-density ratio  $\log \frac{\pi_b(a|s)}{\pi_i(a|s)}$ ,

where  $\pi_i(a|s)$  is the current policy and  $\pi_b(a|s)$  refers to the behavioral prior policy to stay close to. Next we derive the policy losses corresponding to linear scalarization and DiME in this application setting, where a single scalar  $\alpha \in [0, 1]$  specifies the preference trade-off between these two objectives.

## 5.1 Kickstarting

In kickstarting, the behavioral prior is a policy  $\pi_b$  that we can use to evaluate the density  $\pi_b(a|s)$ . Thus the log-density ratio can be evaluated point-wise. As mentioned in Section 3.3, linear scalarization corresponds to simply using a convex combination of these two objectives and applying the projection in (2), which leads to:

$$J_{\text{LS}}(\theta) = \mathbb{E}_{\substack{s \sim \mu \\ a \sim \pi_i}} \left[ \frac{1}{Z_0(s)} \exp \left( (1 - \alpha) \frac{Q(s, a)}{\eta} + \frac{\alpha}{\eta} \log \frac{\pi_b(a|s)}{\pi_i(a|s)} \right) \log \pi_\theta(a|s) \right]. \quad (8)$$

Similarly, substituting the  $q_k(a|s)$ , introduced in Section 4, into the projection of (3), produces the following policy objective:

$$J_{\text{DiME}}(\theta) = \mathbb{E}_{\substack{s \sim \mu \\ a \sim \pi_i}} \left[ \left( \frac{(1 - \alpha)}{Z_1(s)} \exp \left( \frac{Q(s, a)}{\eta_1} \right) + \frac{\alpha}{Z_2(s)} \exp \left( \frac{\log \frac{\pi_b(a|s)}{\pi_i(a|s)}}{\eta_2} \right) \right) \log \pi_\theta(a|s) \right]. \quad (9)$$

The normalizing constants above, denoted  $Z_*(s)$ , normalize the product of  $\pi_i$  and the corresponding exponentiated and tempered objective. Though analytically intractable, these can be estimated from sampled actions for each state. Finally, note that both of the equations above are equivalent at the extreme values of  $\alpha = 0$  and 1.

## 5.2 Offline RL

In offline RL, the behavioral prior is a dataset of transitions  $(s, a, r, s')$ , so we cannot evaluate the density  $\pi_b(a|s)$  and thus cannot query the proximity objective function. Instead, we must simplify both  $J_{\text{LS}}$  and  $J_{\text{DiME}}$  so that they only rely on sampling from  $\pi_b$ .

**Linear scalarization.** If we tie the preference trade-off and scale parameter  $\alpha = \eta$  in (8) we obtain

$$J_{\text{LS}}(\theta) = \mathbb{E}_{\substack{s \sim \mu \\ a \sim \pi_i}} \left[ \frac{\pi_b(a|s)}{\pi_i(a|s)} \frac{1}{Z_0(s)} \exp \left( \frac{(1 - \alpha)}{\alpha} Q(s, a) \right) \log \pi_\theta(a|s) \right]. \quad (10)$$

After cancelling out and rearranging terms, the expectation is now over the following distribution, for which the given dataset is a sample:

$$= \mathbb{E}_{\substack{s \sim \mu \\ a \sim \pi_b}} \left[ \exp \left( \frac{Q(s, a)}{\beta} - \log Z_0(s) \right) \log \pi_\theta(a|s) \right], \quad (11)$$

where  $\beta = \alpha/(1 - \alpha)$  corresponds to the the temperature hyperparameter used in offline RL algorithms such as CRR and AWAC. There are close similarities between this policy objective that relies on linear scalarization, and other policy losses used in recent literature, e.g., CRR, AWAC, ABM, REQ, and AWR [52, 28, 46, 18, 37, resp.]. For example, we can recover CRR by replacing the task return objective from the Q-function with the advantage function  $A(s, a) = Q(s, a) - V(s)$  (which corresponds to approximating  $\log Z_0(s) = V(s)/\beta$  above).

**DiME.** If we set  $\eta_2 = 1$  and rename  $\eta = \eta_1$  in (9), we obtain

$$J_{\text{DiME}}(\theta) = (1 - \alpha) \mathbb{E}_{\substack{s \sim \mu \\ a \sim \pi_i}} \left[ \frac{1}{Z_1(s)} \exp \left( \frac{Q(s, a)}{\eta} \right) \log \pi_\theta(a|s) \right] + \alpha \mathbb{E}_{\substack{s \sim \mu \\ a \sim \pi_b}} [\log \pi_\theta(a|s)]. \quad (12)$$

Notice that the first term is the loss used by policy optimization methods such as REPS [38] and MPO [1], and the second term is exactly a behavioral cloning loss. This is a simple way of adapting online RL algorithms for offline RL.

**Remarks.** There are two main drawbacks to the linear scalarization approach. First, the preference parameter  $\alpha$  and scale parameter  $\eta$  can no longer be set independently—they are coupled together in the temperature parameter  $\beta$ . Second, since  $J_{\text{LS}}$  only involves an expectation with respect to the expert behavior policy, the policy cannot evaluate and exploit the Q-value estimates for actions beyond those taken by the expert. One could argue that this is by design, in order to avoid fitting extrapolation errors in the Q-function. However, with  $J_{\text{DiME}}$  this a choice we can make (perhaps adaptively) and independently from the parameter  $\eta$ , which regularizes the policy optimization.

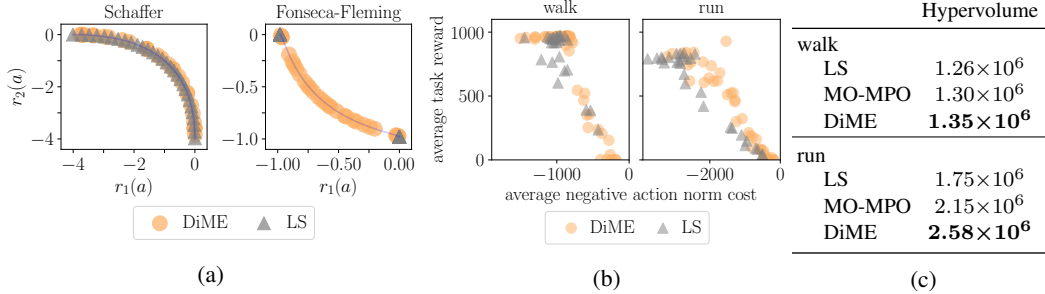


Figure 1: Each point is a solution found for a different tradeoff  $\{\alpha_k\}$ . (a) DiME can find solutions on a concave Pareto front (Fonseca-Fleming, right) whereas linear scalarization (LS) cannot. (b) On the humanoid tasks, DiME finds better solutions than LS. Above (i.e., higher task reward) and to the right (i.e., lower cost) indicates better performance. (c) DiME performs best, in terms of hypervolume.

## 6 Experiments

In our empirical evaluation, we first assess the performance of DiME on standard multi-objective RL problems (Sec. 6.1). Then we investigate the application of DiME in two case studies: offline RL (Sec. 6.2) and kickstarting (Sec. 6.3). In the case studies, we aim to compare DiME to the standard approach of optimizing for a linear scalarization of the objectives. For hyperparameter and implementation details, please refer to the appendix.

### 6.1 Multi-Objective RL

We first investigate whether DiME is a strong multi-objective RL approach, by evaluating it on toy domains with known Pareto fronts and on continuous control tasks. We refer to the appendix for further experiments on DiME’s scale invariance.

**Baselines.** We compare against two existing approaches: 1) MO-MPO [2], which is a state-of-the-art multi-objective RL algorithm; and 2) linear scalarization (LS). These two baselines differ from DiME only in terms of the policy improvement step, as explained in Sec. 3.3 and 4.

**Toy Domain.** Our bandit task has action  $a \in \mathbf{R}$  and reward  $r(a) \in \mathbf{R}^2$ , with the reward defined by either the Schaffer or Fonseca-Fleming function [30]. The Pareto front is the set of all points of the function. By varying the trade-off, DiME finds solutions along the entire Pareto front for both functions. However, no matter what the trade-off is, LS only finds solutions at the extremes of Fonseca-Fleming, because this Pareto front is concave (Fig. 1a, right). This is a fundamental limitation of linear scalarization—it cannot find solutions on the concave portions of a Pareto front [7].

**Humanoid.** We also evaluate on two humanoid tasks from the DeepMind Control Suite [48]. For each, the original task reward objective is augmented with an “energy”-expenditure penalty on actions:  $-\|a\|_2$ . In both tasks, the Pareto front found by DiME is superior to that found by LS (Fig. 1b) and on par with MO-MPO (see appendix). In terms of hypervolume, which is a standard metric for capturing the overall quality of a Pareto front, DiME outperforms both LS and MO-MPO (Table 1c).

### 6.2 Offline RL

In the first of two case studies, we investigate using DiME for offline RL, where there are two objectives: maximizing the learned Q-values and staying close to the actions in the dataset.

**Baselines.** In the LS baseline, we use linear scalarization to trade off between the two objectives, capturing the task return objective with the advantage function as discussed above. This baseline optimizes for the policy loss  $\mathbb{E}_{s \sim \mu, a \sim \pi_b} \exp((1-\alpha)/\alpha(Q(s, a) - V(s))) \log \pi_\theta(a|s)$ . LS then has the same policy loss as CRR-exp [52] and AWAC [28], two state-of-the-art offline RL algorithms. In terms of implementation, we share as much as possible with DiME (e.g., learning hyperparameters, network architectures) to make the comparison fair. Finally, the behavioral cloning (BC) baseline optimizes  $\mathbb{E}_{s \sim \mu, a \sim \pi_b} \log \pi_\theta(a|s)$ , which is equivalent to both methods with  $\alpha = 1$ .

| Task                    | <i>BCQ</i> | <i>BRAC</i> | <i>CRR</i> † | <i>MZU</i> | BC    | LS<br>(CRR)  | DiME<br>(BC) | DiME<br>(AWBC) | DiME<br>(BC)<br>multi | DiME<br>(AWBC)<br>multi |
|-------------------------|------------|-------------|--------------|------------|-------|--------------|--------------|----------------|-----------------------|-------------------------|
| cartpole swingup        | 445        | <b>869</b>  | 664          | 343        | 379.6 | <b>843.4</b> | <b>881.9</b> | <b>880.6</b>   | <b>880.2</b>          | <b>881.3</b>            |
| cheetah run             | 369        | 539         | 577          | <b>799</b> | 375.8 | 796.3        | 733.2        | 759.0          | <b>840.7</b>          | <b>806.4</b>            |
| finger turn hard        | 174        | 227         | 714          | 405        | 132.2 | 515.4        | <b>884.6</b> | <b>891.8</b>   | <b>895.8</b>          | <b>927.5</b>            |
| fish swim               | 384        | 222         | 517          | 585        | 492.9 | 613.1        | 651.9        | 668.6          | <b>724.2</b>          | 674.6                   |
| humanoid run            | 23         | 10          | 586          | <b>633</b> | 390.1 | <b>635.4</b> | <b>637.6</b> | <b>660.0</b>   | 614.2                 | <b>664.5</b>            |
| manipulator insert ball | 98         | 56          | 625          | 557        | 369.5 | 603.4        | 651.6        | 625.9          | <b>680.7</b>          | <b>693.0</b>            |
| manipulator insert peg  | 54         | 50          | 387          | 433        | 261.2 | 409.9        | 385.6        | 434.8          | 388.9                 | <b>457.9</b>            |
| walker stand            | 502        | 829         | 797          | 760        | 286.1 | 706.2        | <b>954.8</b> | <b>951.3</b>   | <b>950.1</b>          | <b>973.1</b>            |
| walker walk             | 661        | 786         | 901          | 902        | 361.0 | 867.9        | <b>955.3</b> | <b>956.5</b>   | <b>965.1</b>          | <b>970.4</b>            |

| Task                   | <i>BRAC</i> | <i>BEAR</i> | <i>AWR</i> | <i>BCQ</i> | <i>CQL</i> | BC   | LS<br>(CRR) | DiME<br>(BC)<br>multi | DiME<br>(AWBC)<br>multi |
|------------------------|-------------|-------------|------------|------------|------------|------|-------------|-----------------------|-------------------------|
| antmaze umaze          | 0.7         | 0.7         | 0.6        | 0.8        | 0.7        | 0.42 | <b>0.97</b> | <b>0.99</b>           | <b>0.95</b>             |
| antmaze umaze diverse  | 0.7         | 0.6         | 0.7        | 0.6        | 0.8        | 0.45 | <b>0.88</b> | 0.83                  | <b>0.86</b>             |
| antmaze medium play    | 0           | 0           | 0          | 0          | 0.6        | 0.02 | <b>0.87</b> | <b>0.86</b>           | <b>0.86</b>             |
| antmaze medium diverse | 0           | 0.1         | 0          | 0          | 0.5        | 0.01 | <b>0.95</b> | 0.90                  | <b>0.91</b>             |
| antmaze large play     | 0           | 0           | 0          | 0.1        | 0.2        | 0    | <b>0.87</b> | 0.62                  | <b>0.87</b>             |
| antmaze large diverse  | 0           | 0           | 0          | 0          | 0.1        | 0    | 0.78        | 0.51                  | <b>0.83</b>             |
| kitchen complete       | 0           | 0           | 0          | 0.3        | 1.8        | 2.18 | <b>3.09</b> | <b>2.99</b>           | 2.63                    |
| kitchen partial        | 0           | 0.5         | 0.6        | 0.8        | 1.9        | 1.77 | 1.93        | <b>2.08</b>           | 1.67                    |
| kitchen mixed          | 0           | 1.9         | 0.4        | 0.3        | 2.0        | 2.32 | <b>2.46</b> | <b>2.58</b>           | 2.08                    |

Table 1: Results for LS and DiME (average cumulative reward) obtained for the best tradeoff per algorithm, on tasks from RL Unplugged (above) and D4RL (below). For RL Unplugged, the results for BC, BCQ, and BRAC are from Gulcehre et al. [13]; CRR is from Wang et al. [52], referred to as ‘‘CRR exp’’ in their paper; and MZU (MuZero Unplugged) is from Schrittwieser et al. [45]. For D4RL, the results for the italicized algorithms are taken from Fu et al. [8]; these are the best-performing algorithms from their comprehensive evaluation. Numbers within 5% of the best score are in bold. †Note that the CRR results are computed by selecting the best checkpoint throughout training, whereas all other results denote performance after a fixed number of learning steps.

**Variations of DiME.** For offline RL, DiME optimizes for (12), where the second term is a behavior cloning loss. DiME enables the flexibility to replace this term with a different way of measuring closeness to the dataset. So, we also consider using an advantage-weighted behavior cloning loss,  $\mathbb{E}_{\pi_b(a|s)}[\exp(A(s, a)) \log \pi_\theta(a|s)]$ , which is exactly the CRR policy loss with a temperature of 1. We evaluate both options, DiME (BC) and DiME (AWBC). We also experiment with a trade-off-conditioned policy  $\pi_\theta(a|s, \alpha)$ , to avoid having to train a separate policy per trade-off. For this, trade-offs are sampled uniformly in  $[0, 1]$  during training. Then, at test time, we rollout this policy for different fixed tradeoffs. We refer to this as DiME multi, and combine it with both BC and AWBC.

**Evaluation.** We use tasks from two offline RL benchmarks: RL Unplugged [13] and D4RL [8]. We train policies for one million learner steps with the tradeoff  $\alpha$  linearly spaced from 0.05 to 1.

From RL Unplugged, we evaluate on the nine Control Suite tasks. For both LS and DiME, the setting of  $\alpha$  has a significant impact on performance, and the optimal setting is different per task (Fig. 2). Comparing the best performance obtained for each task (across parameter settings), both DiME (BC) multi and DiME (AWBC) multi outperform LS (Table 1, above). Empirically, it seems training a single tradeoff-conditioned policy is not only more efficient, but also leads to better performance. This may be because conditioning on  $\alpha$  regularizes learning. We also trained  $\alpha$ -conditioned policies for LS, but this did not work well; possibly because in LS,  $\alpha$  controls both the tradeoff, and scaling.

From D4RL, we evaluate on the six Ant Maze tasks and three Franka Kitchen tasks. We only evaluate the DiME multi variants, since they perform well on the Control Suite tasks. On the D4RL tasks, LS and DiME perform on par, and both outperform current state-of-the-art approaches (Table 1, below).



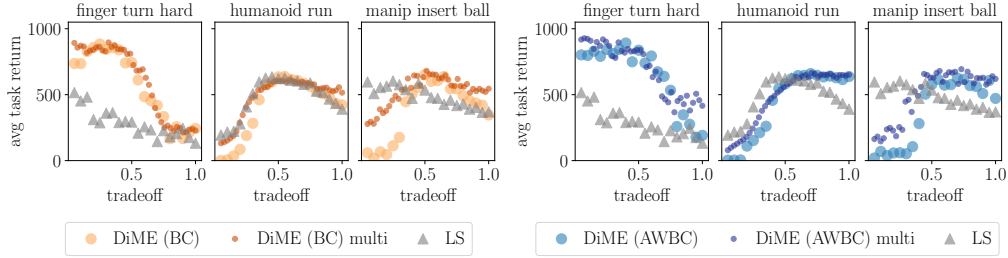


Figure 2: Per-tradeoff performance for a representative subset of tasks; the appendix contains plots for all fifteen tasks. On some tasks, the best solution found by DiME (any variation) obtains significantly higher task performance than the best found by LS. In addition, DiME can train a *single* policy for a range of tradeoffs (DiME multi, dark orange and dark blue), that performs comparably to learning a separate policy for each tradeoff (orange and blue), after the same number of learning steps.

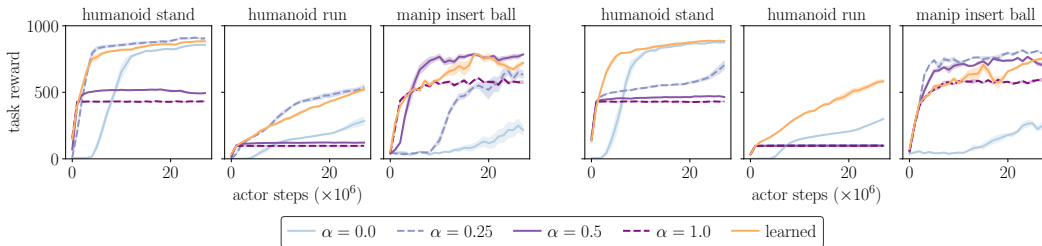


Figure 3: Learning curves for kickstarting, for DiME (left three) and LS (right three). (The appendix contains plots for all five tasks.)  $\alpha = 1$  means fully imitating the behavioral prior, while  $\alpha = 0$  means learning from scratch. The optimal fixed tradeoff  $\alpha$  depends on the task. For both DiME and LS, learning the tradeoff (orange) converges to better performance than fully imitating the behavioral prior (dashed purple), while learning as quickly. Error bars show standard error across three seeds.

Table 1 also includes numbers from prior work (left side). These are given for reference but are not directly comparable; due to differences in network architectures and the fact that LS and DiME use different temperatures per task (chosen via a grid-search). But as can be seen, our LS outperforms these references and thus serves as a strictly improved baseline—and when compared to reference CRR results, this highlights the importance of selecting an appropriate temperature.

### 6.3 Kickstarting

In the second case study, we apply DiME to kickstarting. We train policies from scratch, with guidance from a behavioral prior that we can query for the density  $\pi_b(a|s)$ . This behavioral prior could be a policy learned via offline RL; this is in fact how we obtain  $\pi_b$  for the manipulator tasks.

We evaluate LS and DiME, as described in Sec. 5.1, with either a fixed or learned tradeoff. To learn the tradeoff, we update  $\alpha$  based on the loss  $J(\alpha) = \alpha (\mathbb{E}_{s \sim \mu, a \sim \pi_i(\cdot|s)} Q(s, a) - c)$ . This is analogous to the update for the Lagrange multiplier in Lagrangian relaxation for constrained optimization. The result is intuitive: stay close to the behavioral prior while expected return is below the threshold  $c$ , and otherwise optimize for the bootstrapped Q-function. We pick  $c$  based on the expected return from fully imitating the prior for the given task (i.e.,  $\alpha = 1$ ); these values are given in the appendix.

We evaluate on the humanoid and manipulator tasks from the DeepMind Control Suite. For the three humanoid tasks, we start with a suboptimal humanoid stand policy as the behavioral prior. For the two manipulator tasks, the behavioral prior is a policy trained for that task.

The choice of fixed tradeoff impacts the result significantly, and the optimal choice depends on the task, so either searching over or learning the tradeoff is necessary. For example, for DiME, the best fixed tradeoff is 0.25 for the humanoid tasks and 0.5 for the manipulator tasks (Fig. 3, left). Interestingly, for LS, on the humanoid tasks none of the fixed tradeoffs outperform learning from scratch (i.e.,  $\alpha = 0$ ) (Fig. 3, right). This is because of the difference in the objective functions' scales—a more fine-grained search of tradeoffs between 0 and 0.25 is necessary.

Across all five tasks, for both LS and DiME, the learned tradeoff converges to better performance than fully imitating the prior ( $\alpha = 1$ ) and learns much more quickly than learning from scratch ( $\alpha = 0$ ). This requires training only a single policy, as opposed to training a separate policy per fixed tradeoff.

## 7 Conclusion and Future Work

In this work, we looked at multi-objective optimization as a tool for tackling challenges in RL. We explored the benefits of this perspective in two case studies, offline RL and kickstarting, both of which involve staying close to a behavioral prior. We revealed that existing approaches optimize for a linear scalarization of two objectives, task return and a log-density ratio, and proposed a new algorithm, DiME, that provides a flexible alternative. Applying DiME to offline RL leads to state-of-the-art performance on two benchmarks. A key takeaway is the impact of the trade-off parameter  $\alpha$  on performance, and the need to either search over or optimize for it. As a first solution we explored training trade-off-conditioned policies and adapting the trade-off during training. As with any deep RL algorithm, there are potential negative (and positive) societal impacts in how this work is applied.

## 8 Acknowledgements

The authors would like to thank Philemon Brakel, Francis Song, Brendan Tracey, Markus Wulfmeier, Andrea Huber, Leslie Fritz, the Control Team, and many others at DeepMind for their helpful feedback and support for this paper.

## References

- [1] Abbas Abdolmaleki, Jost Tobias Springenberg, Yuval Tassa, Remi Munos, Nicolas Heess, and Martin Riedmiller. Maximum a posteriori policy optimisation. In *Proceedings of the Sixth International Conference on Learning Representations (ICLR)*, 2018.
- [2] Abbas Abdolmaleki, Sandy H. Huang, Leonard Hasenclever, Michael Neunert, Francis Song, Martina Zambelli, Murilo F. Martins, Nicolas Heess, Raia Hadsell, and Martin Riedmiller. A distributional view on multi-objective policy optimization. In *Proceedings of the 37th International Conference on Machine Learning (ICML)*, 2020.
- [3] Gabriel Barth-Maron, Matthew W. Hoffman, David Budden, Will Dabney, Dan Horgan, Dhruva TB, Alistair Muldal, Nicolas Heess, and Timothy Lillicrap. Distributional policy gradients. In *International Conference on Learning Representations (ICLR)*, 2018.
- [4] Marc Bellemare, Sriram Srinivasan, Georg Ostrovski, Tom Schaul, David Saxton, and Remi Munos. Unifying count-based exploration and intrinsic motivation. In *Advances in Neural Information Processing Systems*, 2016.
- [5] Marc G. Bellemare, Will Dabney, and Rémi Munos. A distributional perspective on reinforcement learning. *CoRR*, abs/1707.06887, 2017. URL <http://arxiv.org/abs/1707.06887>.
- [6] Tim Brys, Anna Harutyunyan, Halit Bener Suay, Sonia Chernova, Matthew E. Taylor, and Ann Nowé. Reinforcement learning from demonstration through shaping. In *Proceedings of the 24th International Conference on Artificial Intelligence (IJCAI)*, 2015.
- [7] I. Das and J. E. Dennis. A closer look at drawbacks of minimizing weighted sums of objectives for pareto set generation in multicriteria optimization problems. *Structural Optimization*, 14: 63–69, 1997.
- [8] Justin Fu, Aviral Kumar, Ofir Nachum, George Tucker, and Sergey Levine. D4rl: Datasets for deep data-driven reinforcement learning. *arXiv preprint arXiv:2004.07219*, 2020.
- [9] Scott Fujimoto, David Meger, and Doina Precup. Off-policy deep reinforcement learning without exploration. In Kamalika Chaudhuri and Ruslan Salakhutdinov, editors, *Proceedings of the 36th International Conference on Machine Learning*, volume 97 of *Proceedings of Machine Learning Research*, pages 2052–2062. PMLR, 09–15 Jun 2019. URL <http://proceedings.mlr.press/v97/fujimoto19a.html>.

- [10] Alexandre Galashov, Siddhant M. Jayakumar, Leonard Hasenclever, Dhruva Tirumala, Jonathan Schwarz, Guillaume Desjardins, Wojciech M. Czarnecki, Yee Whye Teh, Razvan Pascanu, and Nicolas Heess. Information asymmetry in KL-regularized RL. In *Proceedings of the 7th International Conference on Learning Representations (ICLR)*, 2019.
- [11] Dibya Ghosh, Marlos C. Machado, and Nicolas Le Roux. An operator view of policy gradient methods. *CoRR*, abs/2006.11266, 2020. URL <https://arxiv.org/abs/2006.11266>.
- [12] Daniel Golovin and Qiuyi Zhang. Random hypervolume scalarizations for provable multi-objective black box optimization. In *Proceedings of the 37th International Conference on Machine Learning (ICML)*, 2020.
- [13] Caglar Gulcehre, Ziyu Wang, Alexander Novikov, Thomas Paine, Sergio Gómez, Konrad Zolna, Rishabh Agarwal, Josh S Merel, Daniel J Mankowitz, Cosmin Paduraru, Gabriel Dulac-Arnold, Jerry Li, Mohammad Norouzi, Matthew Hoffman, Nicolas Heess, and Nando de Freitas. RL unplugged: A suite of benchmarks for offline reinforcement learning. In *Advances in Neural Information Processing Systems*, 2020.
- [14] Tuomas Haarnoja, Aurick Zhou, Pieter Abbeel, and Sergey Levine. Soft actor-critic: Off-policy maximum entropy deep reinforcement learning with a stochastic actor. In *Proceedings of the 35th International Conference on Machine Learning (ICML)*, 2018.
- [15] Nicolas Heess, Dhruva TB, Srinivasan Sriram, Jay Lemmon, Josh Merel, Greg Wayne, Yuval Tassa, Tom Erez, Ziyu Wang, S. M. Ali Eslami, Martin Riedmiller, and David Silver. Emergence of locomotion behaviours in rich environments. *arXiv preprint arXiv:1707.02286*, 2017.
- [16] Matt Hoffman, Bobak Shahriari, John Aslanides, Gabriel Barth-Maron, Feryal Behbahani, Tamara Norman, Abbas Abdolmaleki, Albin Cassirer, Fan Yang, Kate Baumli, Sarah Henderson, Alex Novikov, Sergio Gómez Colmenarejo, Serkan Cabi, Caglar Gulcehre, Tom Le Paine, Andrew Cowie, Ziyu Wang, Bilal Piot, and Nando de Freitas. Acme: A research framework for distributed reinforcement learning. *arXiv preprint arXiv:2006.00979*, 2020.
- [17] Max Jaderberg, Volodymyr Mnih, Wojciech Marian Czarnecki, Tom Schaul, Joel Z. Leibo, David Silver, and Koray Kavukcuoglu. Reinforcement learning with unsupervised auxiliary tasks. In *5th International Conference on Learning Representations (ICLR)*, 2017.
- [18] Rae Jeong, Jost Tobias Springenberg, Jackie Kay, Dan Zheng, Alexandre Galashov, Nicolas Heess, and Francesco Nori. Learning dexterous manipulation from suboptimal experts. In *Proceedings of the Conference on Robot Learning (CoRL)*, 2020.
- [19] Dmitry Kalashnikov, Alex Irpan, Peter Pastor, Julian Ibarz, Alexander Herzog, Eric Jang, Deirdre Quillen, Ethan Holly, Mrinal Kalakrishnan, Vincent Vanhoucke, and Sergey Levine. Qt-opt: Scalable deep reinforcement learning for vision-based robotic manipulation. *arXiv preprint arXiv:1806.10293*, 2018.
- [20] Liyiming Ke, Sanjiban Choudhury, Matt Barnes, Wen Sun, Gilwoo Lee, and Siddhartha Srinivasa. Imitation learning as f-divergence minimization. In *Algorithmic Foundations of Robotics XIV*, pages 313–329. Springer International Publishing, 2021.
- [21] Diederik P. Kingma and Jimmy Ba. Adam: A method for stochastic optimization. In *Proceedings of the Third International Conference on Learning Representations (ICLR)*, 2015.
- [22] Sascha Lange, Thomas Gabel, and Martin Riedmiller. Batch reinforcement learning. In *Reinforcement learning*, pages 45–73. Springer, 2012.
- [23] Sergey Levine. Reinforcement learning and control as probabilistic inference: Tutorial and review. *arXiv preprint arXiv:1805.00909*, 2018.
- [24] Volodymyr Mnih, Koray Kavukcuoglu, David Silver, Andrei A Rusu, Joel Veness, Marc G Bellemare, Alex Graves, Martin Riedmiller, Andreas K Fidjeland, Georg Ostrovski, et al. Human-level control through deep reinforcement learning. *Nature*, 518(7540):529, 2015.

- [25] Volodymyr Mnih, Adria Puigdomenech Badia, Mehdi Mirza, Alex Graves, Timothy Lillicrap, Tim Harley, David Silver, and Koray Kavukcuoglu. Asynchronous methods for deep reinforcement learning. In *Proceedings of The 33rd International Conference on Machine Learning*, 2016.
- [26] Kristof Van Moffaert and Ann Nowé. Multi-objective reinforcement learning using sets of Pareto dominating policies. *Journal of Machine Learning Research*, 15:3663–3692, 2014.
- [27] Hossam Mossalam, Yannis M. Assael, Diederik M. Roijers, and Shimon Whiteson. Multi-objective deep reinforcement learning. *arXiv preprint arXiv:1610.02707*, 2016.
- [28] Ashvin Nair, Abhishek Gupta, Murtaza Dalal, and Sergey Levine. Awac: Accelerating online reinforcement learning with offline datasets. *arXiv preprint arXiv:2006.09359*, 2020.
- [29] Andrew Y. Ng, Daishi Harada, and Stuart J. Russell. Policy invariance under reward transformations: Theory and application to reward shaping. In *Proceedings of the Sixteenth International Conference on Machine Learning (ICML)*, 1999.
- [30] Tatsuya Okabe, Yaochu Jin, Markus Olhofer, and Bernhard Sendhoff. On test functions for evolutionary multi-objective optimization. In *Parallel Problem Solving from Nature - PPSN VIII*, 2004.
- [31] OpenAI, Marcin Andrychowicz, Bowen Baker, Maciek Chociej, Rafal Jozefowicz, Bob McGrew, Jakub Pachocki, Arthur Petron, Matthias Plappert, Glenn Powell, Alex Ray, Jonas Schneider, Szymon Sidor, Josh Tobin, Peter Welinder, Lilian Weng, and Wojciech Zaremba. Learning dexterous in-hand manipulation. *arXiv preprint arXiv:1808.00177*, 2018.
- [32] Simone Parisi, Matteo Pirota, and Marcello Restelli. Multi-objective reinforcement learning through continuous pareto manifold approximation. *Journal of Artificial Intelligence Research*, 57:187–227, 2016.
- [33] Simone Parisi, Matteo Pirota, and Jan Peters. Manifold-based multi-objective policy search with sample reuse. *Neurocomputing*, 263:3–14, 2017.
- [34] Emilio Parisotto, Jimmy Lei Ba, and Ruslan Salakhutdinov. Actor-mimic: Deep multitask and transfer reinforcement learning. *arXiv preprint arXiv:1511.06342*, 2015.
- [35] Deepak Pathak, Pulkit Agrawal, Alexei A. Efros, and Trevor Darrell. Curiosity-driven exploration by self-supervised prediction. In *Proceedings of the 34th International Conference on Machine Learning (ICML)*, 2017.
- [36] Xue Bin Peng, Pieter Abbeel, Sergey Levine, and Michiel van de Panne. Deepmimic: Example-guided deep reinforcement learning of physics-based character skills. *ACM Transactions on Graphics*, 37(4), 2018.
- [37] Xue Bin Peng, Aviral Kumar, Grace Zhang, and Sergey Levine. Advantage-weighted regression: Simple and scalable off-policy reinforcement learning. *arXiv preprint arXiv:1910.00177*, 2019.
- [38] Jan Peters, Katharina Mülling, and Yasemin Altun. Relative entropy policy search. In *Proceedings of the Twenty-Fourth AAAI Conference on Artificial Intelligence*, AAAI’10, page 1607–1612. AAAI Press, 2010.
- [39] Mathieu Reymond and Ann Nowé. Pareto-DQN: Approximating the Pareto front in complex multi-objective decision problems. In *Proceedings of the Adaptive and Learning Agents Workshop at the 18th International Conference on Autonomous Agents and MultiAgent Systems AAMAS*, 2019.
- [40] Diederik M. Roijers, Peter Vamplew, Shimon Whiteson, and Richard Dazeley. A survey of multi-objective sequential decision-making. *Journal of Artificial Intelligence Research*, 48(1): 67–113, 2013.
- [41] Diederik M. Roijers, Shimon Whiteson, and Frans A. Oliehoek. Linear support for multi-objective coordination graphs. In *Proceedings of the International Conference on Autonomous Agents and Multi-Agent Systems (AAMAS)*, pages 1297–1304, 2014.

- [42] Stuart Russell and Andrew L. Zimdars. Q-decomposition for reinforcement learning agents. In *Proceedings of the Twentieth International Conference on International Conference on Machine Learning (ICML)*, pages 656–663, 2003.
- [43] Andrei A Rusu, Sergio Gomez Colmenarejo, Caglar Gulcehre, Guillaume Desjardins, James Kirkpatrick, Razvan Pascanu, Volodymyr Mnih, Koray Kavukcuoglu, and Raia Hadsell. Policy distillation. *arXiv preprint arXiv:1511.06295*, 2015.
- [44] Simon Schmitt, Jonathan J. Hudson, Augustin Zidek, Simon Osindero, Carl Doersch, Wojciech M. Czarnecki, Joel Z. Leibo, Heinrich Kuttler, Andrew Zisserman, Karen Simonyan, and S. M. Ali Eslami. Kickstarting deep reinforcement learning. *arXiv preprint arXiv:1803.03835*, 2018.
- [45] Julian Schrittwieser, Thomas Hubert, Amol Mandhane, Mohammadamin Barekatain, Ioannis Antonoglou, and David Silver. Online and offline reinforcement learning by planning with a learned model. *arXiv preprint arXiv:2104.06294*, 2021.
- [46] Noah Y. Siegel, Jost Tobias Springenberg, Felix Berkenkamp, Abbas Abdolmaleki, Michael Neunert, Thomas Lampe, Roland Hafner, Nicolas Heess, and Martin A. Riedmiller. Keep doing what worked: Behavioral modelling priors for offline reinforcement learning. *CoRR*, abs/2002.08396, 2020. URL <https://arxiv.org/abs/2002.08396>.
- [47] D. Silver, A. Huang, C. J. Maddison, A. Guez, L. Sifre, G. van den Driessche, J. Schrittwieser, I. Antonoglou, V. Panneershelvam, M. Lanctot, S. Dieleman, D. Grewe, J. Nham, N. Kalchbrenner, I. Sutskever, T. Lillicrap, M. Leach, K. Kavukcuoglu, T. Graepel, and D. Hassabis. Mastering the game of Go with deep neural networks and tree search. *Nature*, 529:484–503, 2016.
- [48] Yuval Tassa, Yotam Doron, Alistair Muldal, Tom Erez, Yazhe Li, Diego de Las Casas, David Budden, Abbas Abdolmaleki, Josh Merel, Andrew Lefrancq, Timothy Lillicrap, and Martin Riedmiller. Deepmind control suite. *arXiv preprint arXiv:1801.00690*, 2018.
- [49] Gerald Tesauro, Rajarshi Das, Hoi Chan, Jeffrey Kephart, David Levine, Freeman Rawson, and Charles Lefurgy. Managing power consumption and performance of computing systems using reinforcement learning. In *Advances in Neural Information Processing Systems*, pages 1497–1504, 2008.
- [50] Peter Vamplew, Richard Dazeley, Adam Berry, Rustam Issabekov, and Evan Dekker. Empirical evaluation methods for multiobjective reinforcement learning algorithms. *Machine Learning*, 84(1):51–80, Jul 2011.
- [51] Kristof Van Moffaert, Madalina M Drugan, and Ann Nowé. Scalarized multi-objective reinforcement learning: Novel design techniques. In *2013 IEEE Symposium on Adaptive Dynamic Programming and Reinforcement Learning (ADPRL)*, pages 191–199. IEEE, 2013.
- [52] Ziyu Wang, Alexander Novikov, Konrad Zolna, Josh S Merel, Jost Tobias Springenberg, Scott E Reed, Bobak Shahriari, Noah Siegel, Caglar Gulcehre, Nicolas Heess, and Nando de Freitas. Critic regularized regression. In *Advances in Neural Information Processing Systems (NeurIPS)*, 2020.
- [53] Jie Xu, Yunsheng Tian, Pingchuan Ma, Daniela Rus, Shinjiro Sueda, and Wojciech Matusik. Prediction-guided multi-objective reinforcement learning for continuous robot control. In *Proceedings of the 37th International Conference on Machine Learning (ICML)*, 2020.
- [54] Runzhe Yang, Xingyuan Sun, and Karthik Narasimhan. A generalized algorithm for multi-objective reinforcement learning and policy adaptation. In *Proceedings of the 32nd International Conference on Neural Information Processing Systems (NeurIPS)*, pages 14610–14621, 2019.
- [55] Marcela Zuluaga, Andreas Krause, and Markus Püschel.  $\epsilon$ -pal: An active learning approach to the multi-objective optimization problem. *Journal of Machine Learning Research*, 17(1): 3619–3650, 2016.

## A Training Trade-off-conditioned Policies

In this section we provide details on training a trade-off-conditioned policy  $\pi_\theta(a|s, \alpha)$  conditioned on preference parameters  $\alpha \sim \nu(\alpha)$ . (Note that here  $\alpha$  corresponds exactly to  $\underline{\alpha}$  from the main body of this manuscript; we had to distinguish it from the single scalar that appears in our case studies, but we drop the underline here to lighten notation.) Conditioning the policy on the trade-off  $\alpha$  requires that the Q-functions are also trade-off-conditioned. We also use hindsight relabeling of trade-offs to perform off-policy learning.

**Preference-conditioned policy evaluation.** We evaluate the current policy  $\pi_i(a|s, \alpha)$  via off-policy learning of per-objective Q-functions  $Q_k^i(s, a, \alpha)$ . When training the Q-network, every sampled transition  $(s, a, \{r_k\}_{k=1}^K, s')$  is augmented such that the states include a sampled trade-off parameter  $\alpha \sim \nu$ , resulting in transitions  $([s, \alpha], a, \{r_k\}_{k=1}^K, [s', \alpha])$ . From here, any critic learning algorithm can be used; we use distributional Q-learning [5, 3]. See Section C for more details.

**Preference-conditioned policy improvement.** The policy improvement step produces a trade-off-conditioned policy  $\pi_{i+1}(a|s, \alpha)$  that improves upon its predecessor  $\pi_i$ .

*Improvement:* To find per-objective improved action distributions  $q_k(a|s, \alpha)$ , we optimize the following policy optimization problem for each objective:

$$\max_{q_k} \mathbb{E}_{\substack{s \sim \mu \\ \alpha \sim \nu}} [\mathbb{E}_{a \sim q_k(\cdot|s, \alpha)} Q_k^i(s, a, \alpha)] \quad (13)$$

$$\text{s.t. } \mathbb{E}_{\substack{s \sim \mu \\ \alpha \sim \nu}} \text{KL}(q_k(a|s, \alpha) \| \pi_i(a|s, \alpha)) \leq \epsilon_k. \quad (14)$$

Similarly, from here we can follow steps analogous to those in Section B, but with trade-off-conditioned policies and Q-functions. This means that this set of trade-off-conditioned problems have solutions that are analogous to (39) for each objective.

*Projection:* After obtaining per-objective improved policies  $q_k$ , we can use supervised learning to distill these distributions into a new parameterized policy:

$$\max_{\theta} \mathbb{E}_{\substack{s \sim \mu \\ \alpha \sim \nu}} \sum_{k=1}^K \alpha_k \text{KL}(q_k(\cdot|s, \alpha) \| \pi_\theta(\cdot|s, \alpha)) \quad (15)$$

$$\text{s.t. } \mathbb{E}_{\substack{s \sim \mu \\ \alpha \sim \nu}} [\text{KL}(\pi_i(\cdot|s, \alpha) \| \pi_\theta(\cdot|s, \alpha))] \leq \beta,$$

subject to a trust region with bound  $\beta > 0$  for more stable learning. To solve this optimization, we use Lagrangian relaxation as described in Abdolmaleki et al. [1, 2].

**In practice.** To approximate the expectations over the state and trade-off distribution distributions, we draw states from a dataset (or replay buffer in online RL) and augment each with a sampled trade-off  $\alpha \sim \nu$ . To approximate the integrals over actions  $a$ , for each  $(s, \alpha)$  pair we sample  $N$  actions from the current policy  $\pi_i(a|s, \alpha)$ .

## B Multi-Objective RL as Probabilistic Inference

In this section we present further details of our derivation, which unifies both linear scalarization and DiME, relying on the *RL as inference* framework. We begin by recalling some of the motivation behind the objective.

Consider a set of binary random variables  $R_k$  indicating a policy improvement event with respect to objective  $k$ ;  $R_k = 1$  indicates that our policy has improved for objective  $k$ , while  $R_k = 0$  indicates that it has not. We seek a policy that improves with respect to *all* objectives given some preferences over objectives. Concretely, we seek policy parameters  $\theta$  that maximize the following marginal likelihood, given preference trade-off coefficients  $\{\alpha_k\}$ :

$$\max_{\theta} \mathbb{E}_{\mu} \log p_{\theta}(\{R_k = 1\}_{k=1}^K | \{\alpha_k\}_{k=1}^K). \quad (16)$$

Assuming independence between improvement events  $R_k$  we use the following model to enforce trade-offs between objectives, i.e.,

$$F(\theta) = \mathbb{E}_{\mu} \log \prod_{k=1}^K p_{\theta}(R_k | s)^{\alpha_k} = \sum_{k=1}^K \alpha_k \mathbb{E}_{\mu} \log p_{\theta}(R_k | s). \quad (17)$$

This generalization has a few nice properties. First, when all objectives are equally preferred, the  $\alpha_k$  are all equal and it reduces to a straightforward probabilistic factorization of independent events:  $p(\{R_k\}_{k=1}^K) = \prod_k p(R_k)$ . Second, any vanishing  $\alpha_k$  leads to an objective being ignored.

Consider the intractable marginal likelihood  $L$  that we wish to maximize, then introduce variational distributions  $q_k$  and expand as follows

$$F(\theta) = \sum_{k=1}^K \alpha_k \mathbb{E}_\mu \log p_\theta(R_k|s) \quad (18)$$

$$= \sum_{k=1}^K \alpha_k \mathbb{E}_\mu \mathbb{E}_{q_k} \log p_\theta(R_k|s) \quad (19)$$

$$= \sum_{k=1}^K \alpha_k \mathbb{E}_\mu \mathbb{E}_{q_k} \log \frac{p_\theta(R_k, a|s)}{p_\theta(a|R_k, s)} \quad (20)$$

$$= \sum_{k=1}^K \alpha_k \mathbb{E}_\mu \mathbb{E}_{q_k} \log \frac{q_k(a|s) p_\theta(R_k, a|s)}{p_\theta(a|R_k, s) q_k(a|s)} \quad (21)$$

$$= \sum_{k=1}^K \alpha_k \mathbb{E}_\mu [\text{KL}(q_k(a|s) \| p_\theta(a|R_k, s)) - \text{KL}(q_k(a|s) \| p_\theta(R_k, a|s))] \quad (22)$$

$$= \sum_{k=1}^K \alpha_k \mathbb{E}_\mu [\text{KL}(q_k(a|s) \| p_\theta(a|R_k, s)) - \text{KL}(q_k(a|s) \| p(R_k|s, a)\pi_\theta(a|s))] \quad (23)$$

Let us denote the second term as  $F$ , defined as follows

$$L(\theta; \{q_k\}) := - \sum_{k=1}^K \alpha_k \mathbb{E}_\mu \text{KL}(q_k(a|s) \| p(R_k|s, a)\pi_\theta(a|s)) \quad (24)$$

Then one can rearrange terms in the expansion of the marginal likelihood  $F$  to yield

$$F(\theta) - \sum_{k=1}^K \alpha_k \mathbb{E}_\mu \text{KL}(q_k(a|s) \| p_\theta(a|R_k, s)) = L(\theta; \{q_k\}). \quad (25)$$

Since the KL divergence is a non-negative quantity, this last equation shows that  $L$  lower-bounds the quantity we wish to maximize, namely  $F$ . Whether we call it expectation-maximization or improvement-projection, the steps are as follows:

1. tighten the gap between the lower bound  $L$  and  $F$  at the current iterate  $\theta_i$ , by maximizing  $L$  with respect to  $q_k$  while keeping  $\theta = \theta_i$  fixed, then
2. maximize the lower bound  $L$  with respect to  $\theta$ , holding  $q_k$  fixed to the solution of step 1.

Formally, these two steps result in the following optimization problems

$$\max_{\{q_k\}} L(\theta_i; \{q_k\}) = \min_{\{q_k\}} \sum_{k=1}^K \alpha_k \mathbb{E}_\mu \text{KL}(q_k(a|s) \| p(R_k|s, a)\pi_i(a|s)) \quad (26)$$

$$\max_{\theta} L(\theta; \{q_k\}) = \min_{\theta} \sum_{k=1}^K \alpha_k \mathbb{E}_\mu \text{KL}(q_k(a|s) \| \pi_\theta(a|s)), \quad (27)$$

where in the second step we removed terms that do not depend on  $\theta$ . These steps are respectively referred to as the E- and M-step in the statistics literature, and improvement and projection in policy optimization. While these two optimization problems seem decoupled from the original goal of maximizing  $F$ , the connection with the EM algorithm allows us to enjoy the guarantee that iterates  $\theta_i$  obtained in this way lead to improvements in  $F$ .

## B.1 Improvement or E-step

In the next sections we detail the two steps in turn, beginning with the improvement E-step, where we first notice that the objective is a weighted sum of  $K$  independent terms that can all be minimized separately

$$\operatorname{argmin}_{\{q_k\}} \sum_{k=1}^K \alpha_k \mathbb{E}_\mu \operatorname{KL}(q_k(a|s) \| p(R_k|s, a)\pi_i(a|s)) \quad (28)$$

$$\Leftrightarrow \operatorname{argmin}_{q_k} \mathbb{E}_\mu \operatorname{KL}(q_k(a|s) \| p(R_k|s, a)\pi_i(a|s)), \quad \forall k = 1, \dots, K. \quad (29)$$

These separate problems can be solved analytically by making the KL vanish with the following solution

$$q_k(a|s) = \frac{p(R_k|s, a)\pi_i(a|s)}{\int \pi_i(a|s)p(R_k|s, a) da} \quad (30)$$

This nonparametric distribution reweights the actions based on the improvement likelihood  $p(R_k|s, a)$ . This likelihood is free for us to model as follows and as is standard in the *RL as inference* literature

$$p(R_k|s, a) \propto \exp \frac{Q_k(s, a)}{\eta_k}, \quad (31)$$

where  $\eta_k$  is a objective-dependent temperature parameter that controls how greedy the solution  $q_k(a|s)$  is with respect to its associated objective  $Q_k(s, a)$ . Substituting this choice of  $p(R_k|s, a)$  into the independent problems (29) we obtain the following objective

$$\operatorname{KL}(q_k(a|s) \| p(R_k|s, a)\pi_i(a|s)) = \mathbb{E}_{q_k} \log \frac{q_k(a|s)}{p(R_k|s, a)\pi_i(a|s)} \quad (32)$$

$$= \mathbb{E}_{q_k} \left[ \log \frac{q_k(a|s)}{\pi_i(a|s)} - \log p(R_k|s, a) \right] \quad (33)$$

$$= \operatorname{KL}(q_k(a|s) \| \pi_i(a|s)) - \mathbb{E}_{q_k} \log p(R_k|s, a), \quad (34)$$

$$= \operatorname{KL}(q_k(a|s) \| \pi_i(a|s)) - \mathbb{E}_{q_k} \frac{Q_k(s, a)}{\eta_k}. \quad (35)$$

After multiplying this objective by  $-\eta_k$ , we obtain the following equivalent maximization problem

$$\max_{q_k} \mathbb{E}_\mu \mathbb{E}_{q_k} Q_k(s, a) - \eta_k \mathbb{E}_\mu \operatorname{KL}(q_k(a|s) \| \pi_i(a|s)), \quad (36)$$

where we recognize a KL regularization term that materializes naturally from this derivation. Indeed this last optimization problem can be seen as a Lagrangian, imposing a soft constraint on the KL between the improved policy  $q_k$  and the current iterate  $\theta_i$ . If we instead impose a hard such constraint, we obtain the following problem:

$$\begin{aligned} \max_{q_k} \quad & \mathbb{E}_\mu \mathbb{E}_{q_k} Q_k(s, a) \\ \text{s.t.} \quad & \mathbb{E}_\mu \operatorname{KL}(q_k(a|s) \| \pi_i(a|s)) \leq \epsilon_k. \end{aligned} \quad (37)$$

This problem's Lagrangian form is as follows, and is nearly identical to (36)—albeit with a different dual variable instead of  $\eta_k$ ; nevertheless we reuse the notation  $\eta_k$  instead of introducing a new dual variable:

$$\mathcal{L}(q_k, \eta_k) = \mathbb{E}_\mu \mathbb{E}_{q_k} Q_k(s, a) - \eta_k [\mathbb{E}_\mu \operatorname{KL}(q_k(a|s) \| \pi_i(a|s)) - \epsilon_k]. \quad (38)$$

**Putting everything together.** Since the original problem is equivalent to the Lagrangian relaxation of this one, we can simply substitute our improvement likelihood (31) into the solution to the original problem (30) to obtain the solution:

$$q_k(a|s) = \frac{1}{Z_k(s)} \pi_i(a|s) \exp \frac{Q_k(s, a)}{\eta_k}, \quad \text{where} \quad (39)$$

$$Z_k(s) = \int \pi_i(a|s) \exp \frac{Q_k(s, a)}{\eta_k} da. \quad (40)$$



**Adaptively varying  $\eta_k$ .** Finally, this solution can in turn be substituted back into (38) to obtain the following convex dual function:

$$\mathcal{L}^*(\eta_k) = \mathbb{E}_\mu \mathbb{E}_{q_k} Q_k(s, a) + \eta_k \mathbb{E}_\mu \left[ \epsilon_k - \mathbb{E}_{q_k} \log \frac{\frac{1}{Z_k(s)} \pi_i(a|s) \exp \frac{Q_k(s, a)}{\eta_k}}{\pi_i(a|s)} \right] \quad (41)$$

$$= \mathbb{E}_\mu \mathbb{E}_{q_k} Q_k(s, a) + \eta_k \mathbb{E}_\mu \left[ \epsilon_k - \mathbb{E}_{q_k} \log \left( \frac{1}{Z_k(s)} \exp \frac{Q_k(s, a)}{\eta_k} \right) \right] \quad (42)$$

$$= \mathbb{E}_\mu \mathbb{E}_{q_k} Q_k(s, a) + \eta_k \mathbb{E}_\mu \left[ \epsilon_k + \log Z_k(s) - \mathbb{E}_{q_k} \frac{Q_k(s, a)}{\eta_k} \right] \quad (43)$$

$$= \mathbb{E}_\mu \mathbb{E}_{q_k} Q_k(s, a) + \eta_k \mathbb{E}_\mu [\epsilon_k + \log Z_k(s)] - \mathbb{E}_\mu \mathbb{E}_{q_k} Q_k(s, a) \quad (44)$$

$$= \eta_k [\epsilon_k + \mathbb{E}_\mu \log Z_k(s)] \quad (45)$$

$$\mathcal{L}^*(\eta_k) = \eta_k \left[ \epsilon_k + \mathbb{E}_\mu \log \mathbb{E}_{\pi_i} \exp \frac{Q_k(s, a)}{\eta_k} \right], \quad (46)$$

where in the final step we substitute (40) to reveal the hidden dual variable. In practice, this function is optimized alongside of  $\theta$  in order to adapt the dual variable  $\eta_k$  and mitigate overfitting to  $Q_k$ .

## B.2 Projection or M-step

Let us now look at the projection step (M-step in EM terminology), which produces the next iterate  $\theta_{i+1}$  for our parametric policy. Recall the optimization problem involved in the M-step is the following

$$\min_{\theta} L(\theta; q_k) = \min_{\theta} \sum_{k=1}^K \alpha_k \mathbb{E}_\mu \text{KL}(q_k(a|s) \parallel \pi_\theta(a|s)), \quad (47)$$

$$= \min_{\theta} \sum_{k=1}^K \alpha_k \mathbb{E}_\mu \mathbb{E}_{q_k} \log \pi_\theta(a|s), \quad (48)$$

where  $q_k$  is fixed to the solution from the improvement step, namely (39). This problem corresponds to finding the policy  $\pi_\theta$  that acts as a barycentre between the nonparametric policies  $q_k$ , each weighted by its specified preference trade-off coefficient  $\alpha_k$ .

Other than this important difference, the multi-objective follows from the single-objective case in a straightforward way. Substituting the solution  $q_k$  from (39) into the expression for  $L(\theta; q_k)$  yields

$$J_{\text{DiME}}(\theta) := L(\theta; q_k) = \mathbb{E}_\mu \left[ \sum_{k=1}^K \alpha_k \mathbb{E}_{q_k} \log \pi_\theta(a|s) \right] \quad (49)$$

$$= \mathbb{E}_\mu \left[ \sum_{k=1}^K \alpha_k \int \frac{1}{Z_k(s)} \pi_i(a|s) \exp \frac{Q_k(s, a)}{\eta_k} \log \pi_\theta(a|s) da \right] \quad (50)$$

$$= \mathbb{E}_\mu \left[ \sum_{k=1}^K \frac{\alpha_k}{Z_k(s)} \mathbb{E}_{\pi_i} \exp \frac{Q_k(s, a)}{\eta_k} \log \pi_\theta(a|s) \right] \quad (51)$$

$$= \mathbb{E}_\mu \mathbb{E}_{\pi_i} \left[ \sum_{k=1}^K \frac{\alpha_k}{Z_k(s)} \exp \frac{Q_k(s, a)}{\eta_k} \right] \log \pi_\theta(a|s). \quad (52)$$

This is the objective function that is optimized to obtain the next iterate in practice. At this stage we can further impose a trust-region or soft KL constraint on this optimization problem.

**In practice.** We compute this policy objective via Monte Carlo, sampling states  $s$  from a replay buffer, then sampling actions for each state from our previous iterate  $\pi_i$ . We use these samples to compute weights  $\exp(Q_k(s, a)/\eta_k)$  and normalize them across states, which corresponds to using a sample-based approximation to  $Z_k(s)$  as well. Finally, we take the convex combination of these weights, according to the preference trade-offs, which yields the ultimate weights—seen in brackets in (52).

## C Implementation Details

This section describes how we implemented our algorithm, DiME, and the linear scalarization (LS) and behavioral cloning (BC) baselines. To ensure a fair comparison, we use the same hyperparameters and network architectures for DiME and the baselines, wherever possible. All algorithms are implemented in Acme [16], an open-source framework for distributed RL.

**Training Setup.** For the multi-objective RL and kickstarting settings, we use an asynchronous actor-learner setup, with multiple actors. In this setup, actors fetch policy parameters from the learner and act in the environment, storing those transitions in the replay buffer. The learner samples batches of transitions from the replay buffer and uses these to update the policy and Q-function networks. For the offline RL setting, the dataset of transitions is given and fixed (i.e., there are no actors) and the learner samples batches of transitions from that dataset.

To stabilize learning, we use the common technique of maintaining a target network for each trained network. These target networks are used for computing gradients. Every fixed number of steps, the target network’s weights are updated to match the online network’s weights. For optimization, we use Adam [21]. For the offline RL experiments, we use Adam with weight decay to stabilize learning.

**Gathering Data.** The actors gather data and store it in the replay buffer. When the policy is conditioned on trade-offs, the trade-off is fixed for each episode. In other words, at the start of each episode, the actor samples a trade-off  $\alpha'$  from the distribution  $\nu$ , and acts based on  $\pi(a|s, \alpha')$  for the remainder of the episode. At the start of the next episode, the actor samples a different trade-off, and repeats.

**Hyperparameters and Architecture.** The policy and Q-function networks are feed-forward networks, with an ELU activation after each hidden layer. For both, after the first hidden layer, we add layer normalization followed by a hyperbolic tangent (tanh); we found that this improves stability of learning. The policy outputs a Gaussian distribution with a diagonal covariance matrix.

The default hyperparameters we use in our experiments are reported in Table 2; setting-specific hyperparameters are reported in Table 3.

**Distributional Q-learning.** For our policy evaluation we use a distributional Q-network, C51 [5]. It has proven to be a very effective critic in actor-critic methods for continuous control [3, 16]. We use the exact same training procedure as published and in open-source implementations [3, 16], i.e.,  $n$ -step return bootstrap targets and a projected cross-entropy loss. See Table 2 under Q-learning for our chosen hyperparameters.

**Evaluation.** We evaluate a deterministic policy, by using the mean of the output Gaussian distribution rather than sampling from it. When we evaluate a trade-off-conditioned policy, we condition it on trade-offs linearly spaced from 0.05 to 1.0. For each trade-off  $\alpha'$ , we perform several rollouts where we execute the mean action from  $\pi(a|s, \alpha')$ . Recall that this trade-off specifies a convex combination for two objectives.

For the multi-objective RL experiments, all policies are evaluated after 500 million actor steps. For offline RL, all policies are evaluated after 1 million learner steps.

**Learned Trade-off for Kickstarting.** In our kickstarting experiments, the learned trade-off is passed through the sigmoid function (i.e.,  $1/(1 + \exp(-x))$ ) to ensure it is bounded between 0 and 1.

## D Experiments: Details and Additional Results

This section provides details regarding our experiment domains, as well as additional experiments and plots.

### D.1 Multi-Objective RL

#### D.1.1 Toy Domain

Our toy domain is a bandit with a continuous action  $a \in \mathbb{R}$ . The reward  $r(a) \in \mathbb{R}^2$  is specified by either the Schaffer function or the Fonseca-Fleming function,  $f : \mathbb{R} \mapsto \mathbb{R}^2$ . Each point along this

| Category                     | Hyperparameter                                     | Default                             |
|------------------------------|----------------------------------------------------|-------------------------------------|
| training setup               | batch size                                         | 512                                 |
|                              | number of actors                                   | 4                                   |
|                              | replay buffer size                                 | $3 \times 10^{-7}$                  |
|                              | target network update period                       | 100                                 |
|                              | Adam learning rate                                 | $10^{-4}$                           |
| policy & Q-function networks | layer sizes                                        | (1024, 1024, 1024, 1024, 1024, 512) |
| Q-learning                   | support                                            | $[-150, 150]$                       |
|                              | number of atoms                                    | 101                                 |
|                              | n-step returns                                     | 5                                   |
|                              | discount $\gamma$                                  | 0.99                                |
| policy loss                  | actions sampled per state                          | 30                                  |
|                              | KL-constraint on $q_k(a s), \epsilon_k$            | 0.1                                 |
|                              | KL-constraint on policy mean, $\beta_\mu$          | 0.0025                              |
|                              | KL-constraint on policy covariance, $\beta_\Sigma$ | $10^{-5}$                           |
|                              | initial temperature $\eta$                         | 10                                  |
|                              | Adam learning rate (for dual variables)            | $10^{-2}$                           |

Table 2: Default hyperparameters for all approaches, with decoupled KL-constraint on mean and covariance of the policy M-step.

| Multi-Objective RL |                                                    |                                                                                                                |
|--------------------|----------------------------------------------------|----------------------------------------------------------------------------------------------------------------|
| training setup     | number of actors                                   | 32                                                                                                             |
|                    | replay buffer size                                 | $10^6$                                                                                                         |
|                    | target network update period                       | 200                                                                                                            |
| experiment setup   | trade-offs (DiME)                                  | $\alpha_{\text{task}} = 1$<br>$\alpha_{\text{penalty}} \in \text{linspace}(0.3, 1.5)$                          |
|                    | trade-offs (MO-MPO)                                | $\epsilon_{\text{task}} = 0.1$                                                                                 |
|                    | humanoid walk                                      | $\epsilon_{\text{penalty}} \in \text{linspace}(0, 0.3)$                                                        |
|                    | humanoid run                                       | $\epsilon_{\text{penalty}} \in \text{linspace}(0, 0.15)$                                                       |
|                    | trade-offs (LS)                                    | $\alpha_{\text{task}} = 1 - \alpha_{\text{penalty}}$<br>$\alpha_{\text{penalty}} \in \text{linspace}(0, 0.15)$ |
| policy loss        | actions sampled per state                          | 20                                                                                                             |
|                    | KL-constraint on policy mean, $\beta_\mu$          | 0.001                                                                                                          |
|                    | KL-constraint on policy covariance, $\beta_\Sigma$ | $10^{-7}$                                                                                                      |
| Offline RL         |                                                    |                                                                                                                |
| training setup     | Adam weight decay (RL Unplugged)                   | 0.999999                                                                                                       |
|                    | Adam weight decay (D4RL)                           | 0.99999                                                                                                        |
| experiment setup   | trade-offs                                         | $\alpha \in \text{linspace}(0.005, 1)$                                                                         |
|                    | trade-off distribution, $\nu$                      | $\mathcal{U}(0.005, 1)$                                                                                        |
| policy loss        | KL-constraint $\epsilon$ (LS)                      | 0.01                                                                                                           |
|                    | KL-constraint $\epsilon$ (RL Unplugged)            | 0.5                                                                                                            |
|                    | KL-constraint $\epsilon$ (Kitchen)                 | 0.001                                                                                                          |
|                    | KL-constraint $\epsilon$ (Maze, DiME multi)        | 0.5 (BC), 0.01 (AWBC)                                                                                          |
| Kickstarting       |                                                    |                                                                                                                |
| training setup     | batch size                                         | 1024                                                                                                           |
| experiment setup   | initial trade-off (for learned trade-offs)         | 0.5                                                                                                            |

Table 3: Hyperparameters that are either setting-specific or differ from the defaults in Table 2.

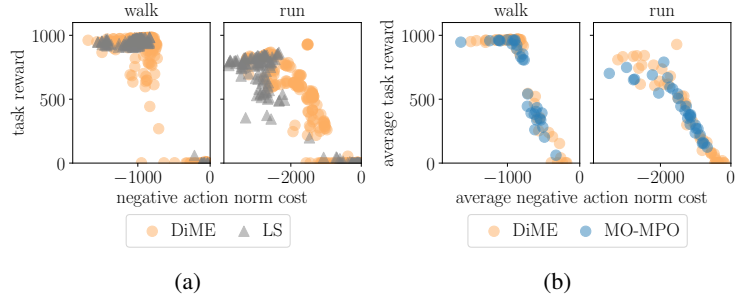


Figure 4: (a) This plot shows the per-episode task reward and action norm cost, rather than the average across episodes. Note that the linear scalarization (LS) cannot find solutions along the Pareto front for walk, because it is likely concave. In contrast, DiME can find solutions that compromise between the two objectives. (b) DiME finds similar Pareto fronts as MO-MPO, a state-of-the-art multi-objective RL algorithm.

function is optimal for a particular tradeoff between the two reward objectives, so the function can be seen as a Pareto front.

The Schaffer function corresponds to a convex Pareto front, and is defined as

$$f_1(a) = a^2$$

$$f_2(a) = (a - 2)^2.$$

The Fonseca-Fleming function corresponds to a concave Pareto front, and is defined as

$$f_1(a) = 1 - \exp(-(a - 1)^2)$$

$$f_2(a) = 1 - \exp(-(a + 1)^2).$$

These are standard test functions in multi-objective optimization, where the aim is to minimize them [30]. Since in RL we want to maximize reward, we define the reward to be the negative of these functions.

### D.1.2 Humanoid

We also evaluate on the humanoid walk and run tasks from the open-sourced DeepMind Control Suite [48], with the two objectives proposed in Abdolmaleki et al. [2]. The first objective is the original task reward, which is a shaped reward that is given for moving at a target speed (1 meters per second for walking and 10 m/s for running), in any direction. The second objective is the negative  $\ell_2$ -norm of the actions,  $-||a||_2$ , which can be seen as encouraging the agent to be more energy-efficient.

The observations are 67-dimensional, consisting of joint angles, joint velocities, center-of-mass velocity, head height, torso orientation, and hand and feet positions. The actions are 21-dimensional and in  $[-1, 1]$ ; these correspond to setting joint accelerations. Each episode has 1000 timesteps. At the start of every episode, the configuration of the humanoid is randomly initialized.

**Additional Results.** When we plot the per-episode performance (rather than an average across episodes), we see that linear scalarization only finds solutions at the two extremes for the humanoid walk task, i.e. policies that achieve high task reward but with high action norm cost, or incur zero cost but fail to obtain any reward (Fig. 4a). We hypothesize that this may be because the humanoid walk task has a concave Pareto front of solutions; recall that linear scalarization is fundamentally unable to find solutions on a concave Pareto front [7]. In contrast, DiME is able to find solutions that trade off between the two objectives.

On both tasks, DiME finds a similar Pareto front as MO-MPO, which is a state-of-the-art approach for multi-objective RL (Fig. 4b).

DiME requires training a separate policy per trade-off, which can be computationally expensive. In contrast, our trade-off-conditioned version of DiME, which we call DiME multi, trains a *single* policy for a range of trade-offs. This obtains a similar Pareto front compared to that found by DiME (Fig. 5), after the same number of actor steps (500 million).

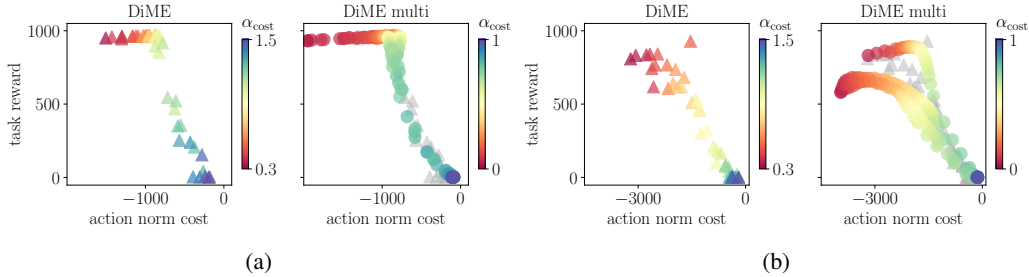


Figure 5: DiME multi trains a single trade-off-conditioned policy, that finds a similar Pareto front as DiME does for humanoid (a) walk and (b) run. Each plot for DiME multi shows five trained policies, for different random seeds; these seeds vary somewhat in their performance because the policy learns different strategies (e.g., spinning, running sideways, etc.). Each policy is conditioned on trade-offs  $\alpha$  linearly spaced between 0 and 1. The color denotes the trade-off. For DiME,  $\alpha_{\text{task}} = 1$ ; DiME multi uses a convex combination (i.e.,  $\alpha_{\text{task}} = 1 - \alpha_{\text{cost}}$ ).

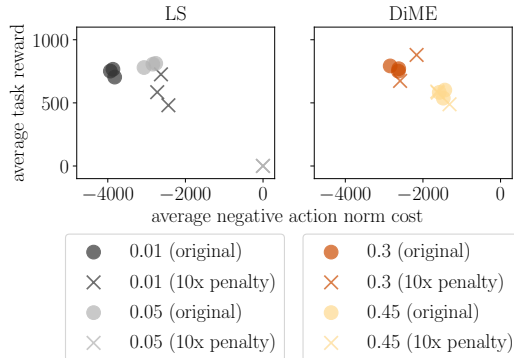


Figure 6: With the original objective scales for humanoid run, both linear scalarization (left plot) and DiME (right) obtain similar performance. When the action norm cost is scaled up by ten times, DiME’s performance is unaffected because its trade-off setting is invariant to reward scales—note the two clusters of differently-colored points. The color denotes the tradeoff  $\alpha$  and the marker symbol denotes whether the action norm cost is scaled by ten times. Note that in the plots, the y-axis is the unscaled value of action norm cost.

We also ran an experiment to test the scale-invariance of DiME. We modified the humanoid run task such that the action norm cost is now multiplied by ten. We used DiME and linear scalarization to train policies for three random seeds, for each of two trade-off settings. For both the original task and the task with scaled-up action norm costs, DiME trains policies with similar performance (Fig. 6, right). This is the case for both trade-off settings—note the two clusters of differently-colored points in the plot. In contrast, linear scalarization is not scale-invariant: task performance suffers when the cost is scaled up (Fig. 6, left). With a trade-off of 0.05, although this obtains better performance than the trade-off of 0.01 with the original objectives (i.e., gets higher reward with lower cost), with the scaled-up action norm cost, policies do not obtain any task reward at all with a trade-off of 0.05.

## D.2 Offline RL

In our offline RL experiments, we evaluate on two open-sourced benchmarks for offline RL: RL Unplugged [13] and D4RL [8]. We use the nine Control Suite tasks from RL Unplugged, the six Ant Maze tasks from D4RL, and the three Franka Kitchen tasks from D4RL. For each task, we train policies on the dataset of transitions provided by the benchmark. These are continuous control tasks, that include particularly challenging ones that state-of-the-art approaches perform poorly on (e.g., Ant Maze large play and large diverse). For a comprehensive description of the environments, please refer to Gulcehre et al. [13] and Fu et al. [8].

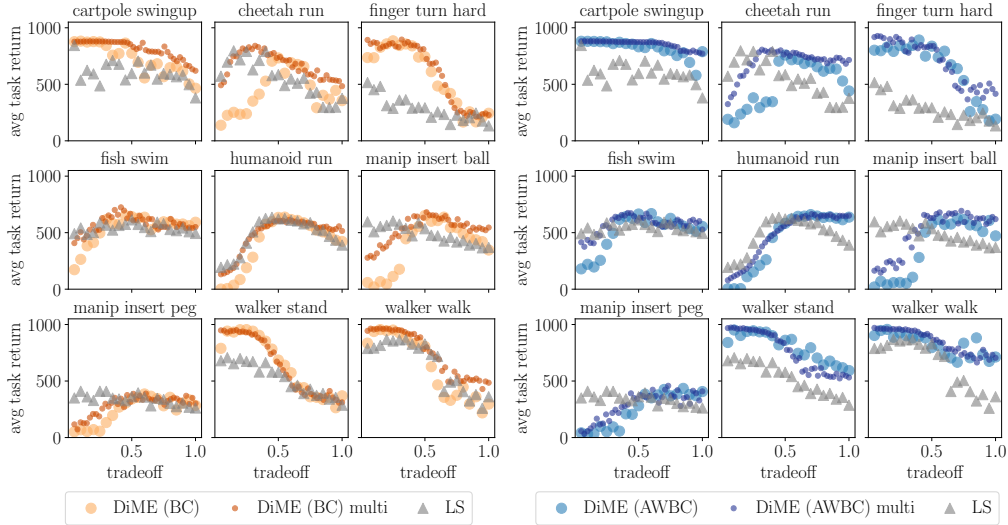


Figure 7: Per-tradeoff performance for all nine Control Suite tasks from RL Unplugged. Across all nine tasks, the best solution found by DiME (any variation) obtains either higher or on-par task performance than the best found by linear scalarization (LS). In addition, DiME can train a *single* policy for a range of tradeoffs (DiME multi, dark orange and dark blue), that performs comparably to learning a separate policy for each tradeoff (orange and blue), after the same number of learning steps.

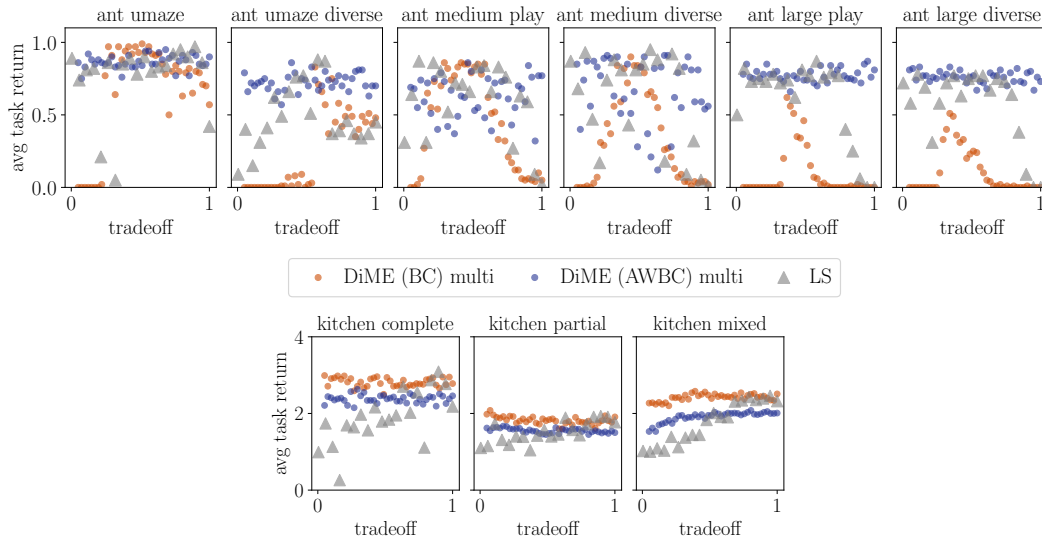


Figure 8: Across nine tasks from D4RL, DiME and LS (CRR) perform on-par.

**Additional Results.** Here we show plots for per-tradeoff performance for all nine Control Suite tasks from RL Unplugged (Fig. 7) and for the Ant Maze and Franka Kitchen tasks from D4RL (Fig. 8). Across all 18 tasks, the best tradeoff found by DiME obtains either higher or on-par performance compared to the best tradeoff found by LS. Recall that LS is equivalent to CRR, a state-of-the-art approach for offline RL, in terms of the policy loss it optimizes for.

### D.3 Kickstarting

For kickstarting, we evaluate on three humanoid tasks (stand, walk, and run) and two manipulator tasks (insert ball and insert peg) from the DeepMind Control Suite. There are two main differences between kickstarting and offline RL: 1) in kickstarting the policy is able to interact with the environment, whereas in offline RL it cannot, and 2) in kickstarting the behavioral prior is in the form of a teacher

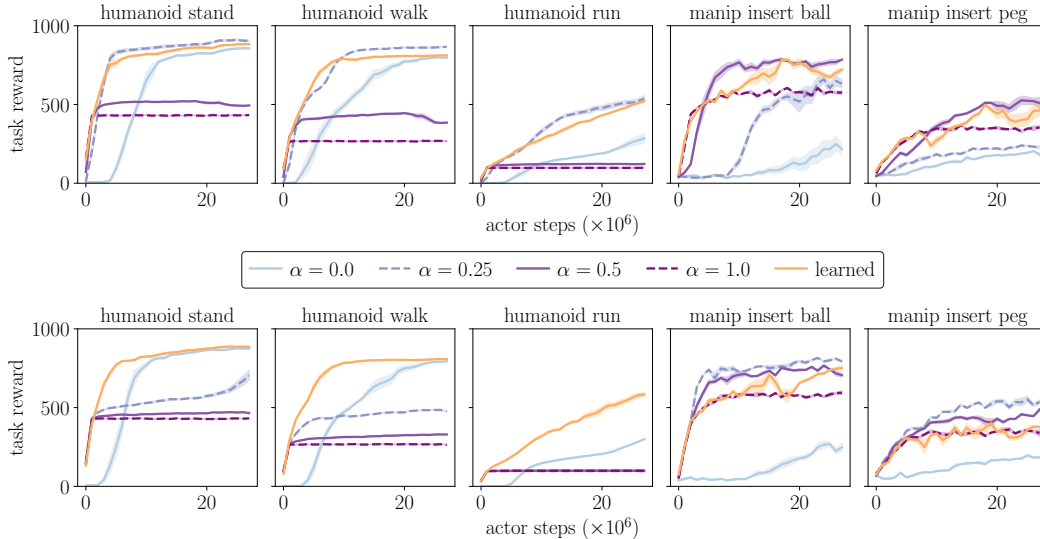


Figure 9: Learning curves for kickstarting, for DiME (top row) and linear scalarization (LS, bottom row).  $\alpha = 1$  corresponds to fully imitating the behavioral prior, while  $\alpha = 0$  corresponds to learning from scratch. The optimal fixed tradeoff  $\alpha$  depends on the task. For both DiME and LS, learning the tradeoff (orange) converges to better performance than fully imitating the behavioral prior (dashed purple), while learning as quickly. The error bars show standard error across three seeds.

policy that we can query to obtain  $\pi_b(a|s)$ , whereas in offline RL the behavior prior is in the form of a dataset of transitions.

For the humanoid tasks, we trained a policy for humanoid stand with standard deep RL (using MPO [1]) and stopped it midway through training, when it reached an average task reward of about 400. We then used this teacher policy for kickstarting in all three humanoid tasks. However, for the manipulator tasks, training a policy from scratch is highly sample-inefficient, as can be seen by the learning curves for learning from scratch (i.e.,  $\alpha = 0$ ) in Fig. 9. So for manipulator insert ball and insert peg, we took the best policy trained using DiME in our offline RL experiments, and used that as the teacher policy for kickstarting in that task.

Fig. 9 shows learning curves for all five tasks. When the tradeoff is learned (in orange), DiME and linear scalarization perform on-par. However, when the tradeoff is fixed, for linear scalarization it is more difficult to pick an appropriate tradeoff, because the appropriate tradeoff depends on the relative scales of the rewards. In fact, for the humanoid tasks, none of the fixed (non-zero) tradeoffs for LS perform better than learning from scratch.